J Appl Electrochem (2007) 37:1375–1381
DOI 10.1007/s10800-007-9397-y

ORIGINAL PAPER

Surface characterization of zincated aluminium and selected alloys at the early stage of the autocatalytic electroless nickel immersion process

Enam Khan · C. F. Oduoza · T. Pearson

Received: 7 March 2007 / Revised: 25 July 2007 / Accepted: 14 August 2007 / Published online: 8 September 2007

Abstract In this work the changing structure of nickel–phosphorus deposits on aluminium and its alloys at the early stage of electroless nickel phosphorus deposition using hypophosphite ion as reducing agent has been studied. Prior to electroless nickel deposition, zincating is used for pre-treatment of aluminium substrates. The surface morphology and structure of the electroless Ni–P layers were characterized by scanning electron microscopy and X-ray diffraction analysis. Results show that Ni–P deposition is closely related to the dissolution of the zincating layer, followed by progressive nickel nucleation. The nuclei serve as a catalytic surface for further Ni–P deposition which increases with deposition time. The growth and coalescence of the nuclei on the aluminium substrate results in crystalline layers of Ni–P.

Keywords Electroless nickel–Phosphorus deposition (Ni–P) · Zincating · Pre-treatment

1 Introduction

Electroless nickel–phosphorus deposition is now an established industrial practice as a protective and decorative coating in various industries due to its superior corrosion and wear resistance, excellent uniformity, wide range of thickness as well as mechanical and physical properties. Extensive research has been carried out on the characterization of the electroless nickel deposition process. Corrosion properties of electroless Ni–P deposition depend mainly on phosphorus content and the corresponding structural and mechanical state. Microporosity, roughness and inhomogeneties due to internal stress within the Ni–P deposited layer are affected by the substrate pre-treatment method. Following Brenner and Riddell [1], there have been many advances in the electroless nickel coating process including the development of ternary alloys and composite coatings.

It is always difficult to plate aluminium and its alloys with any metal or metallic base surface coating, either by a cathodic or electroless deposition due to the tenacious oxide layer present on aluminium. Aluminium and its alloys have high affinity for oxygen which results in a rapidly growing thin oxide film on freshly cleaned and etched aluminium surfaces. It is difficult to plate aluminium substrates covered with such an oxide film with good adhesion. An appropriate pre-treatment process is an essential surface conditioning step before any plating is carried out. The most satisfactory and practical method available for aluminium preparation prior to further deposition is zincating. Zincating is an electrochemical exchange reaction between zinc complexes in solution and the aluminium substrate, depositing zinc crystallites at the expense of aluminium dissolution. The zinc deposition protects the surface, effectively providing a sound basis for subsequent deposition. During the zincating process the aluminium oxide film is first dissolved in zincating solution as follows;

$$Al_2O_3 + 2NaOH + 3H_2O \rightarrow 2NaAl(OH)_4$$

The oxidation of aluminium drives reduction of the zincate ion to produce a layer of zinc metal in a galvanic displacement reaction as follows;

E. Khan · C. F. Oduoza (✉)
School of Engineering & Built Environment, University of Wolverhampton, Telford Campus, Priorslee, Telford TF2 9NT, UK
e-mail: c.f.oduoza@wlv.ac.uk

T. Pearson
MacDermid PlC, Birmingham B9 4EU, UK

$$3Na_2(Zn\,OH)_4 + 2Al_{(substrate)} \rightarrow 2Na\,Al(OH)_4 + 4Na\,OH + 3Zn_{(deposited)}$$

The zincating process usually consists of double dip into the zincate solution to produce a uniform layer of zinc on the aluminium surface. The double zincation protects the aluminium substrate from reoxidation until it is ready to be electrolessly plated with nickel, followed by further deposition.

Electroless nickel deposition is an autocatalytic process in which complexed ions in an aqueous solution are chemically reduced with continued Ni deposition through the catalytic action of the deposit itself. Using sodium hypophosphite reducing agent, the deposited layer always contains phosphorus in addition to nickel. The metallic reduction of nickel is very complex, as the kinetics of the reduction reaction govern not only the rate of metal deposition but also the chemical and physical properties of the electroless nickel deposit. There are numerous parameters affecting the electroless nickel process as suggested by Baudrand [2, 3]. Temperature, pH, nickel ion concentration, reducing agent concentration, the loading in the bath, and agitation will all affect the nickel deposition rate. Brenner and Riddell [1] first developed autocatalytic nickel deposition using a sodium hypophosphite bath. Gutzeit [4, 5] suggested that the nickel ion is catalytically reduced by means of the active atomic hydrogen with simultaneous formation of orthophosphite and hydrogen ions. Gorbunova and Nikiforvoa [6] suggested that atomic hydrogen is released as a result of the catalytic dehydrogenation of hypophosphite molecules adsorbed at the surface which then reduce nickel at the catalyst surface. Electroless nickel deposition therefore cannot be solely chemical but is controlled by an electrochemical mechanism.

The phosphorus content during electroless nickel deposition controls the microstructure of the coating. Previous research on autocatalytic electroless nickel reports that coatings with lower phosphorus content are crystalline and have superior wear resistance while those with higher phosphorus content are amorphous and have superior corrosion resistance. The amorphous nature of the deposits becomes more dominant with increasing phosphorus content. Martyak [7] observed that low phosphorus deposits from an electroless nickel bath were crystalline, while medium phosphorus were more continuous and exhibited a semi-amorphous structure. On the other hand, high phosphorus deposits seemed continuous and amorphous. Kreye et al. [8] and Zhang et al. [9] described electroless nickel coatings with very low phosphorus content as equiaxed and nanocrystalline, while Yamasaki et al. [10], Tyagi et al. [11] and Hur et al. [12], concluded that low phosphorus deposits are crystalline, containing a supersaturated solid solution of phosphorus in the nickel lattice. X-ray diffraction patterns obtained from electroless nickel deposits are known to change with heat treatment as it involves change in microstructure of the nickel matrix [13]. Teheri [14] concluded that the presence of many peaks is evidence of transformation from amorphous and non-crystalline to crystalline structure after heat treatment.

Crystallographic defects due to phosphorus content produce internal stress in the electroless nickel deposits which affect the mechanical and corrosion resistance properties of the coatings. Duncan [15] proposed that the microstructure of electroless Ni–P deposits depends on phosphorus content, as the nature of the internal stress is changed from tensile to compressive with increase in phosphorus content. The structural condition of Ni–P deposition depends on composition, crystallization, and nucleation and growth rate. Deposition with lower phosphorus concentration is characterized by the presence of crystalline and microcrystalline structure, which indicates that the number of phosphorus atoms is not sufficient to distort the nickel lattice. According to Agarwala and Agarwala [16] and Park and Lee [17], an increase in phosphorus content produces amorphous deposition due to the increase in lattice distortion caused by phosphorus atoms situated in the interstitial position of the nickel. It has been found that a number of crystalline non-equilibrium phases are present due to the compositional inhomogeneties prevailing in the Ni–P deposited layer.

2 Experimental procedure

Aluminium alloys Al 1050 and Al 6061 were used as samples for zincating and electroless nickel deposition. These samples were guillotined to size as required for the experiment with the following dimensions: 25 mm × 25 mm × 1 mm for Al 1050 and 25 mm × 25 mm × 1.5 mm for Al 6061, respectively. The chemical composition of Al 1050 and Al 6061 are given in Table 1. Prior to use Al 1050 samples were annealed and strain hardened, while Al 6061 samples were annealed and heat treated [18].

The proprietary Bondal process is a treatment of aluminium and its alloys which enables electrodeposition to be applied without the need for intermediate brass or copper plating. It involves the use of special alkaline cleaners, Minco and Bondal cleaners followed by a unique solution, Bondal dip, containing zinc sulphate, sodium hydroxide, sodium cyanide, nickel sulphate and other additives. The Bondal treatment produces a film on the substrate making it easy to plate directly with nickel and other metals. The concentration and operating conditions were generally based on the Bondal process for plating aluminium and its alloys as recommended by MacDermid [19]. The

Table 1 Chemical composition of aluminium alloys; Al 1050 and Al 6061

Material designation	Chemical composition (%)							
	Si	Fe	Cu	Mn	Mg	Cr	Ti	Zn
Al 1050	0.25	0.40	0.05	0.05	0.05	–	–	0.07
Al 6061	0.2–2.0	0.70	0.1–2.0	0.4–1.5	0.2–1.5	0.05	0.1	0.2–0.25

composition of Minco cleaner at pH > 12, 66-Microetch at pH = 2.0–3.0 and Bondal dip at pH > 12 used were 25–40, 50 and 40 g L^{-1} of water, respectively. The electroless nickel was deposited at the rate of 15–20 μm h^{-1} from commercial solution VAND-ALOY 6000 formulated with sodium hypophosphite as the reducing agent and other additives [20]. The deposits contained 6–9% by weight phosphorus combining high hardness and wear resistance with moderate corrosion resistance.

Pre-treatment and electroless nickel solutions were placed in different sized beakers and provision was made to heat the solution with gentle agitation. The beaker was filled to about two thirds of its volume with deionized water and then filled with VAND-ALOY 6000A (5% by volume) and VAND-ALOY 6000B (15% by volume). The pH of the solution was monitored during immersion and adjusted to the required working range. The solution was then heated to 88–90 °C. Pre-treatment of aluminium was carried out by a displacement process followed by nickel–phosphorus deposition achieved by autocatalytic electroless nickel deposition. The samples were thoroughly rinsed with water after each stage, in order to avoid contamination carried from the previous stage. The sequence of the pre-treatment and electroless nickel plating process onto aluminium is shown in Fig. 1.

Aluminium samples were observed at various relevant stages to study surface morphology and elemental distribution. A ZEISS EVO scanning electron microscope attached to an energy dispersive X-ray spectroscope to facilitate elemental distribution analysis was used for the analysis of deposits at different time intervals. X-ray diffraction was used to study the microstructure, phase identification and orientation of the crystal structure. The crystallographic structures were characterized using a Phillips 1729 X-ray diffractometer with monochromatic CuKα1, CuKα2 radiation of 1.5406, and 1.54439 Å wavelength, respectively, and 40 kV, 40 mA operating power. A scan rate of 0.05° s^{-1} was applied to determine the coating patterns in the 2θ range of 3.0–95.0° of the X-ray diffractometer. Joint Committee of Powder Diffraction Standards (JCPDS) database card file index was used to study the X-Ray diffraction patterns [21].

3 Results and discussion

3.1 Energy dispersive X-ray analysis (EDXA)

EDXA analysis was carried out to investigate the dissolution of zincate coating and to determine the composition of nickel, phosphorus, zinc and other elements during electroless nickel deposition onto Al 1050, Al 6061 at immersion time intervals of 5, 10, 20 and 40 s, 1, 2 and 4 min. There are a variety of opinions as to whether the zinc deposit resulting from zincating is dissolved or not during subsequent electroless nickel processing. Baudrand and Bengston [22] have studied solution formulation and operating conditions influencing adhesion of nickel onto

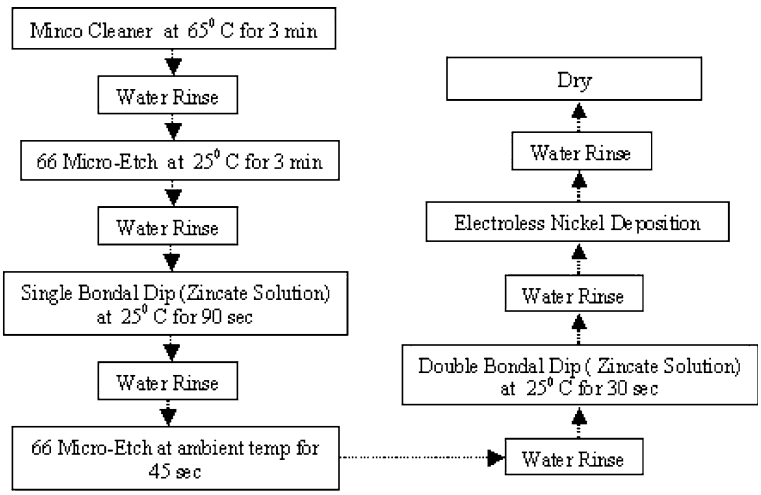

Fig. 1 Process sequence of pre-treatment of aluminium substrate using zincating process (Alkaline cleaning, Acid etch, Desmutting and Bondal dip) and Electroless Nickel deposition

zincated aluminium substrate during electroless nickel deposition. Armyanov [23] concluded that dissolution of the zincate coating is based on plating parameters including pH, temperature, ligand species and concentration. Vangelova et al. [24] have also studied deposits from the acidic electroless nickel solution bath using Auger electron spectroscopy and found that there were no traces of zinc at the aluminium/nickel interface and consequently nickel will be deposited on the aluminium substrate free from oxide film.

Figures 2 and 3 show that, as zinc dissolves, nickel starts to build up on the aluminium surface. Within 60 s of electroless deposition on Al 1050, Ni increases sharply while aluminium is reduced to nearly 5% as shown in Fig. 2a. Other elements such as Zn, Cu, Fe decrease to less than 2% within 2 min of immersion while phosphorus increases as shown in Fig. 2b.

Electroless nickel deposition onto Al 6061 is very similar to that on Al 1050 as shown in Fig. 3a; however, phosphorus increases up to 9% within 4 min as compared to 3% on Al 1050, and Zn, Cu, Fe decrease to less than 2% within 2 min as shown in Fig. 3b.

From EDXA analysis, it has been observed that as zincated aluminium is placed in electroless nickel solution, the film dissolves and there is a replacement of zinc atoms by nickel atoms, which then catalyse further deposition as nickel is reduced by the sodium hypophosphite. It appears that as zincated film is dissolved there is accelerated nucleation, growth and coalescence and then bulk coating with nickel. These results show that Cu, Ni, Fe and Zn are still present on the aluminium substrate during the early stages of electroless immersion and their combined presence, together with the aluminium substrate matrix, all affect nickel deposition.

3.2 Scanning electron microscopy

Figure 4a and b show the surface morphology of the aluminium Al 1050 and Al 6061 after 30 s of double zincating prior to immersion in the electroless nickel bath.

The zincating film is developed by nucleation of crystallites, which partially overlap and multiply, until a smooth zincate layer is formed on the aluminium substrate. The zinc crystallites develop a film with the deposit looking like an island formation. Golby [25], Monterio and Barbosa [26] and Monterio et al. [27] have confirmed that superior adhesion from zincating is associated with uniform, thin, fine-grained films exhibiting rapid and complete surface coverage. Other metals incorporated in the zincate solution are thought to improve the properties of the zincate immersion film [28, 29].

The scanning electron micrograph shown in Fig. 5a after 1 min of electroless deposition shows a significant change on the initial Al 1050 surface. Nickel deposition starts to develop by nucleation after dissolution of the zincated aluminium substrate, as shown in Fig. 5b.

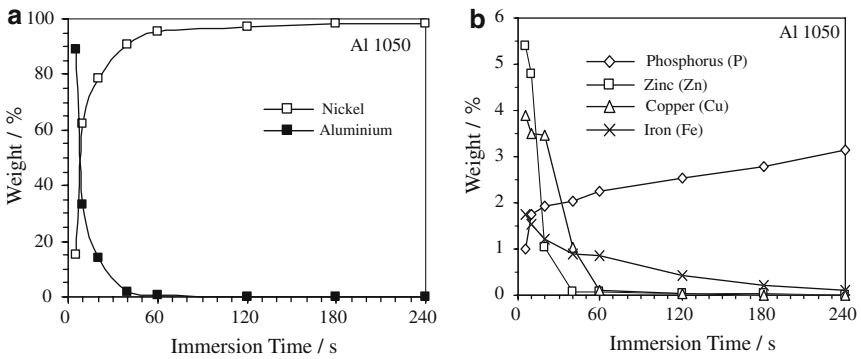

Fig. 2 (**a**) Composition of Al and Ni on Al 1050 substrate after 4 min electroless nickel deposition. (**b**) Composition of P, Zn, Cu and Fe on Al 1050 substrate after 4 min of electroless nickel deposition

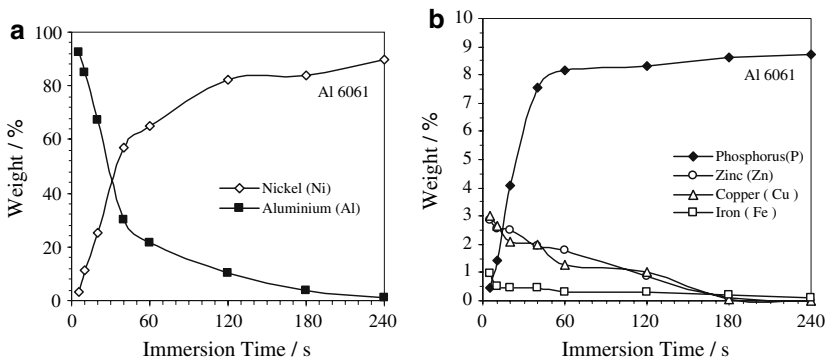

Fig. 3 (**a**) Composition of Al and Ni on Al 6061 substrate after 4 min of electroless nickel deposition. (**b**) Composition of P, Zn, Cu and Fe on Al 6061 substrate after 4 min of electroless nickel deposition

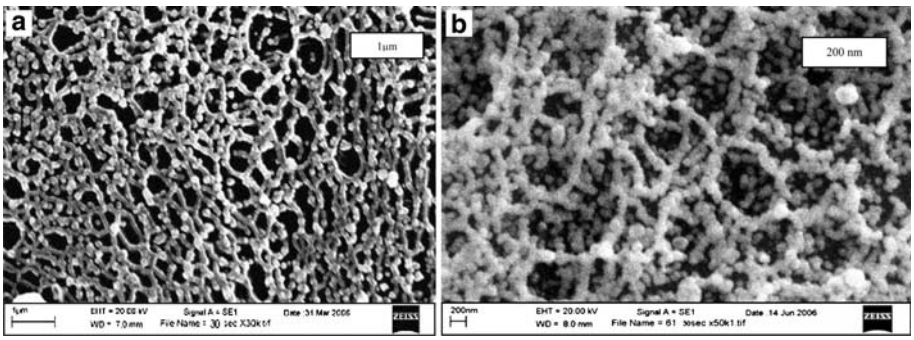

Fig. 4 (**a**) Scanning electron micrograph of Al 1050 after 30 s of double zincating showing island type zincated layer. (**b**) Scanning electron micrograph of Al 6061 after 30 s of double zincating showing island type zincated layer

The deposited nuclei now become catalytic sites for further nickel phosphorus deposition according to Backovic et al. [30]. The growth and coalescence of such nuclei result in a continuous layer of Ni–P on the aluminium surface as shown in Fig. 5c and d after 3 and 4 min of deposition on Al 1050.

The nickel–phosphorus growth continues until nickel has been deposited over almost all the substrate within 4 min of immersion. Although there are still voids on the surface as shown in Fig. 5d, these are filled as autocatalysis continues [31]. The sizes of the nuclei developed, as seen in Fig. 5d and e for Al 1050 and Al 6061, were not of equal size. Al 1050 and Al 6061 were covered by nickel and phosphorus within 4 min of immersion, which confirms the hypothesis that zinc is dissolved during nickel deposition leading to good adhesion for subsequent metal deposition.

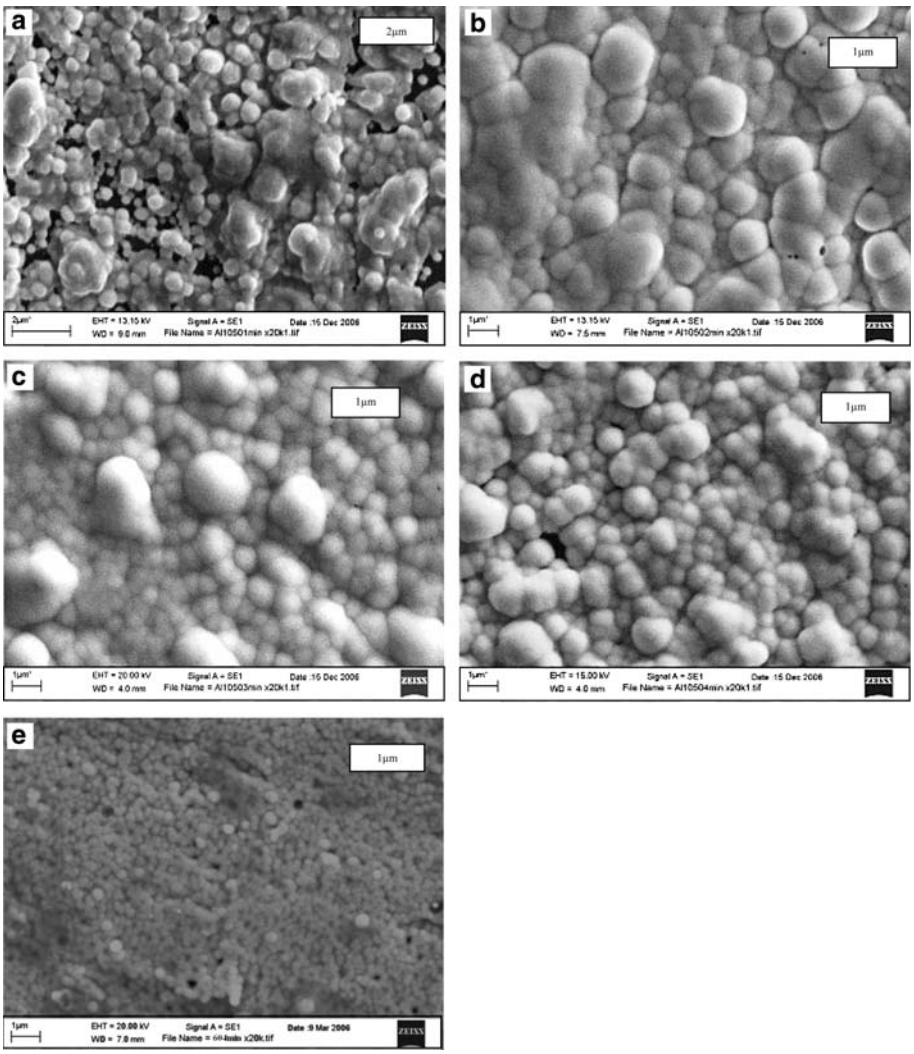

Fig. 5 (**a**) Scanning electron micrograph of Al 1050 surface after 1 min of electroless nickel immersion. (**b**) Scanning electron micrograph of Al 1050 surface after 2 min of electroless nickel immersion. (**c**) Scanning electron micrograph of Al 1050 surface after 3 min of electroless nickel immersion. (**d**) Scanning electron micrograph of Al 1050 surface after 4 min of electroless nickel immersion. (**e**) Scanning electron micrograph of Al 6061 surface after 4 min of electroless nickel immersion

The surface morphology of nickel deposited on Al 6061 as shown in Fig. 5e is dissimilar from that on Al 1050 due to the aluminium alloy matrix affecting the deposition.

3.3 X-Ray diffraction analysis

X-ray diffraction patterns, as shown in Figs. 6 and 7, trace the properties of crystalline and amorphous peaks on Al 1050 and Al 6061. These patterns gradually change from sharp to very broad peaks with increasing phosphorus content as the structural composition slowly changes from crystalline to amorphous. Spectra show sharp peaks around 38°, 44°, 65°, 78° corresponding to nickel and very few diffuse diffraction peaks of varying phases of nickel phosphide Ni_xP_y. There is a possibility that other reflections were present in minor proportions that were not detected because the deposits were too thin. It has been widely observed that fresh bath deposits have either microcrystalline or fine crystalline structures but deviation from crystallinity increase with increase in time and thickness [32]. The sharp diffraction peaks correspond to deposits of crystalline nature while diffuse diffraction peaks reflect amorphous structure.

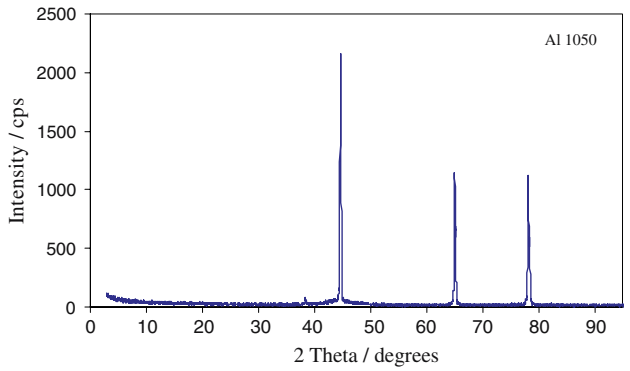

Fig. 6 XRD Patterns of electroless Ni–P deposition on Al 1050 after 4 min of electroless nickel immersion

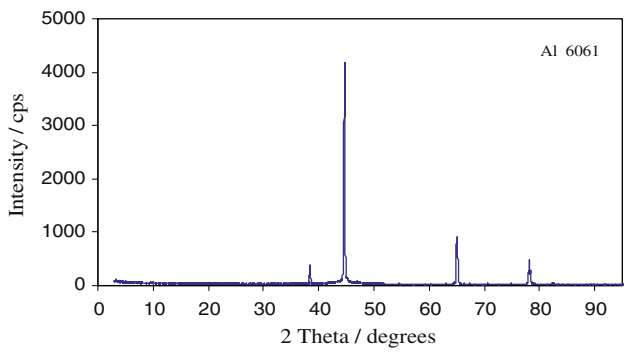

Fig. 7 XRD Patterns of electroless Ni–P deposition on Al 6061 after 4 min of electroless nickel immersion

XRD patterns were obtained after subtracting the background and stripping the CuKα2 lines from the raw data. The Miller indices were measured at 38°, 44°, 65° and 78°. X-ray diffraction measurements made after 10, 20, 40, 60, 120, and 240 s were found to be very similar. X-ray diffraction data in Figs. 6 and 7 were subjected to crystal structural study after 4 min of Ni–P deposition. XRD data processing software [33] and the JCPDS card index file were used to analyse the peaks. The peaks show discrete (hkl) reflections corresponding to face centered cubic and other structures. The XRD pattern for Al 1050, as shown in Fig. 6, reveals a set of distinct textures corresponding to face centered cubic nickel i.e. {111}, {200}, {311}, and {222} after 4 min deposition. These results suggest that crystal planes observed in these textures were grown parallel to the aluminium substrate textures. In the case of Al 6061, textures were different to some extent due to the aluminium alloy matrix. With increasing phosphorus content of the deposits, different textures are developed as {101}, {202}, {222}, {330] after 4 min of electroless deposition on Al 6061, which indicates that the texture development is clearly a function of the phosphorus content. As the phosphorus content in the deposits increases, strain is introduced with a change in the lattice parameters.

The apparent grain sizes of Ni–P alloys were determined using the Scherrer formula [34], which makes use of diffraction broadening. The grain sizes of electroless nickel on Al 1050 and Al 6061 were calculated at 0.576, 0.768 and 1.152 Å full width at half maximum (FWHM). Kreye et al. [8] found that the grain size is usually in the range 2–10 nm. Zhang et al. [9] found grain size varying from 5 to 6 nm, while Randin and Hinterman [35] concluded that average grain size was less than 10 Å. In this study the grain size as deposited from Ni–P was calculated as 2.5 Å [34] for the XRD pattern obtained for Al 1050 and Al 6061.

Lattice constants were obtained by unit cell refinement by applying least squares fitting in the range $10° < 2\theta < 95°$ for Al 1050 and Al 6061 after 1, 2, 3, and 4 min of electroless deposition. Deposition on Al 1050 showed a face centered cubic structure while deposition on Al 6061 portrayed mixed crystal configuration such as face centered cubic, triclinic, tetragonal and monoclinic. These changes in crystal structure with Ni–P deposition are an indication that crystal formation is affected by the presence of the zinc, copper, iron and aluminium alloy matrix even in the early stages of immersion.

4 Conclusions

Zincate treatment of aluminium substrate is an essential pre-treatment step to achieve responsiveness for subsequent electroless nickel plating. SEM and EDXA analyse

have shown that a uniform and dense zincated layer promotes uniform growth of nickel deposits. Elemental distribution results confirm that zinc and other elements present on the substrate surface form complex compounds in the Ni–P bath. Scanning electron microscopy shows that during the initial stages of electroless immersion, a large quantity of nickel is deposited on catalytic centers. However, there is still a fraction of the surface area consisting of voids or gaps between nickel islands. As deposition progresses the gaps become filled due to the self-catalytic nature of the nickel particles.

X-Ray diffraction patterns show sharp, clearly defined peaks of similar intensities on both Al 1050 and Al 6061 after various times of nickel deposition. The X-ray diffraction spectra indicate that the deposited film has a definite crystalline nickel phase. There are other small peaks which are difficult to analyse, but it is clear that they are not nickel rather they appear related to the presence of a Ni_xP_y phase. Crystallization of Ni–P films seem to be affected by the phosphorus content as well as the non-equilibrium conditions of the crystallization process occurring during deposition. The average size of the crystallites within four minutes of electroless Ni–P deposition was calculated to be around 2.5 Å using the Scherrer equation.

Acknowledgements We express our gratitude to the Engineering and Physical Sciences Research Council, UK for the sponsorship of the project and Macdermid PlC for providing some of the materials and equipment used. The authors thank Prof. Craig Williams of the School of Applied Sciences, University of Wolverhampton for his support in the X-ray diffraction analysis.

References

1. Brenner A, Riddell GE (1946) Soc Am Electroplaters 33:23
2. Baudrand D (1979) Plat Surf Finish 66(12):14
3. Baudrand D (1999) Product Finish 63(10):80
4. Gutzeit G (1956) Trans Inst Metal Finish 33:83
5. Gutzeit G (1959) Plat Surf Finish 46:1158, 1275 and 1377
6. Gorbunova KM, Nikiforvoa AA (1963) J Electrochem Soc 110:271c
7. Martyak NM (1994) J Chem Mater Sci 6:1667
8. Kreye H, Muller F, Lang L, Isheim D, Hentschel T (1995) Z Metallkd (Germany) 86:184
9. Zhang YZ, Wu YY, Yao M (1997) J Mater Sci Lett 17:37
10. Yamasaki T, Izumi H, Sunda H (1981) Scripta Metall 15:177
11. Tyagi SVS, Tandon VK, Ray S (1986) J Mater Sci 8:433
12. Hur KH, Jeong JH, Lee DN (1990) J Mater Sci 25:2573
13. Lambert MR, Duquette DJ (1989) Thin Solid films 177:207
14. Teheri R (2003) Doctoral dissertation. University of Saskatchewan, Saskatoon, Canada
15. Duncan RN (1996) Plat Surf Finish 83(65):31
16. Agarwala RC, Agarwala V (2003) Sadhana 28:475
17. Park SH, Lee DN (1988) J Mater Sci 23:1643
18. Aluminium Federation (2003) Aluminium Federation. Birmingham, UK
19. MacDermid plc (2000) Bondal Process, Technical Data Sheet. Birmingham, UK
20. MacDermid plc (2000) VAND-ALOY 6000, Technical Data Sheet Birmingham, UK
21. International Centre for Diffraction Data (1978) JCPDS Card Index File
22. Baudrand D, Bengston J (1995) Metal Finish 93:55
23. Armyanov SA (1992) Metal Finish 90:36
24. Vangelova T, Valova E, Hubnin E, Armyanov SA (2001) J Electrochem Soc Sov Electrochem 148:266
25. Golby JW (1981) Doctoral dissertation. University of Aston, Birmingham, UK
26. Monterio FJ, Barbosa MA (1998) Surf Coat Technol 35:321
27. Monterio FJ, Barbrosa MA, Ross DH, Gabe DR (1991) Surf Interf Anal 17:519
28. Pearson T (2006) Trans Inst Metal Finish 84:121
29. Pearson T, Wake SJ (1997) Trans Inst Metal Finish 75:93
30. Backovic N, Jancic M, Radonjic LJ (1979) Thin Solid Films 59(1):1
31. Libo L, Maozhang A, Gaouhui W (2006) Surf Coat Technol 200:5102
32. Szasz A, Kojnok J, Kertesz L (1984) Thin Solid Films 116:279
33. Dragoe N (2001) J Appl Crystallogr 34:535
34. Rousseau JJ (1998) Basic crystallography. John Wiley & Sons, US
35. Randin J P, Hintermann HE (1967) Plating 54:523